Highly Flexible and Lightweight Organic Solar Cells on Biocompatible Silk Fibroin

ARTICLE *in* ACS APPLIED MATERIALS & INTERFACES · NOVEMBER 2014

Impact Factor: 6.72 · DOI: 10.1021/am504163r · Source: PubMed

9 AUTHORS, INCLUDING:

Liu Yuqiang
Soochow University (PRC)
4 PUBLICATIONS **12** CITATIONS
SEE PROFILE

Ning Qi
Soochow University (PRC)
4 PUBLICATIONS **5** CITATIONS
SEE PROFILE

Zhouhui Xia
Soochow University (PRC)
12 PUBLICATIONS **36** CITATIONS
SEE PROFILE

Baoquan Sun
Soochow University (PRC)
136 PUBLICATIONS **4,690** CITATIONS
SEE PROFILE

ACS APPLIED MATERIALS & INTERFACES

Research Article

www.acsami.org

Highly Flexible and Lightweight Organic Solar Cells on Biocompatible Silk Fibroin

Yuqiang Liu,[†,‡] Ning Qi,[‡] Tao Song,[†] Mingliang Jia,[‡] Zhouhui Xia,[†] Zhongcheng Yuan,[†] Wei Yuan,[‡] Ke-Qin Zhang,*[,‡] and Baoquan Sun*[,†]

[†]Institute of Functional Nano & Soft Materials (FUNSOM), Soochow University, Suzhou, 215123, People's Republic of China

[‡]National Engineering Laboratory for Modern Silk, College of Textile and Clothing Engineering, Research Center of Cooperative Innovation for Functional Organic/Polymer Material Micro/Nanofabrication, Soochow University, Suzhou 215123, People's Republic of China

Supporting Information

ABSTRACT: Organic electronics have gained widespread attention due to their flexibility, lightness, and low-cost potential. It is attractive due to the possibility of large-scale roll-to-roll processing. However, organic electronics require additional development before they can be made commercially available and fully integrated into everyday life. To achieve feasibility for commercial use, these devices must be biocompatible and flexible while maintaining high performance. In this study, biocompatible silk fibroin (SF) was integrated with a mesh of silver nanowires (AgNWs) to build up flexible organic solar cells with maximum power conversion efficiency of up to 6.62%. The AgNW/SF substrate exhibits a conductivity of ∼11.0 Ω/sq and transmittance of ∼80% in the visible light range. These substrates retained their conductivity, even after being bent and unbent 200 times; this surprising ability was attributed to its embedded structure and the properties of the specific SF materials used. To contrast, indium tin oxide on synthetic plastic substrate lost its conductivity after the much less rigid bending. These lightweight and silk-based organic solar cells pave the way for future biocompatible interfaces between wearable electronics and human skin.

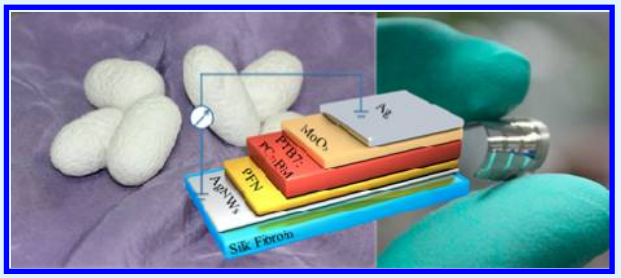

KEYWORDS: *organic solar cells, silk fibroin, flexibility, biocompatible, silver nanowires*

1. INTRODUCTION

Organic solar cells (OSCs) are gaining increasing amounts of attention due to their excellent properties. OSCs are deemed to be one of today's most promising novel photovoltaic devices due to their flexibility, low cost, and large-area manufacturing compatibility.[1,2] OSC flexibility makes them compatible with soft substrates such as garments and textiles.[3] However, for OSCs to be applied onto clothes or other soft surfaces, some of which come into direct contact with skin, they are required to be human-compatible, nontoxic, and nonirritable. The natural silk fibroin (SF), extracted from the silkworm (*Bombyx mori*) cocoon, is a promising alternative material due to its good biocompatibility, biodegradability, nontoxicity, nonirritability, and advantageous mechanical properties,[4] as well as high optical transmittance (90−95%) of films.[5] Furthermore, the biodegradable and mechanical properties of SF substrates can be tailored by controlling the fabrication process such that they match the desired requirements for some specific application.[6−8] For example, SF has been used to fabricate hydrogels, tubes, sponges, fibers, thin films, and other biological composite materials for applications in tissue engineering, drug release carriers, disease models, and implantable devices.[4,9] In particular, this study was inspired by Hwang's work, which showed an organic thin film transistor with a SF-based dielectric layer[10,11] that achieved a high field effect mobility of 23.2 $cm^2V^{-1}s^{-1}$.

In this work, natural SF films were used as substrates in place of glass or synthetic polymers. Silver nanowires (AgNWs) were embedded into SF as a conductive layer. The substrate displayed a conductivity of ∼11 Ω/sq with a transparency of over 80% at 600 nm. An OSC based on a blend of thieno[3,4-*b*]thiophene/benzodithiophene (PTB7) and [6,6]-phenyl-C_{71}-butyric acid methyl ester ($PC_{71}BM$) was fabricated on the SF substrate, achieving a maximum power conversion efficiency (PCE) of 6.62%. A conjugated polymer of poly[(9,9-bis(3′-(*N*,*N*-dimethylamino)propyl)-2,7-fluorene)-*alt*-2,7-(9,9-dioctyl-fluorene)] (PFN) was used to tune the electrical properties of the AgNWs, enhancing their electron collection capability.[12,13] These materials could be effectively functionalized using a spin coating process. The back of the SF films were not exposed to any organic solvents, keeping the biocompatibility properties contained on one side without negatively influence to the whole device.

Received: June 26, 2014
Accepted: November 18, 2014

   dx.doi.org/10.1021/am504163r | *ACS Appl. Mater. Interfaces* XXXX, XXX, XXX−XXX

2. MATERIALS AND METHODS

2.1. Preparation of Conductive Silk Film. Silver nanowires solution (Blue Nano, Inc.) was spin coated onto a clean silicon wafer, and then annealed to form a film of AgNWs. The edge of the AgNWs film was removed by the mechanical exfoliation using tape stickers, obtaining the electrode pattern as shown in Figure S4a (Supporting Information). As shown in Figure 1, the SF solution was fabricated from *Bombyx mori* cocoons. The cocoons were boiled to remove the sericin proteins, dissolved (using LiBr solution), dialyzed (3 days) to remove Li^+ and Br^- then finally subjected to centrifuging to remove impurities. Following this, the SF solution was dropped onto the silver nanowire film. The substrate was carefully removed after the solution dried.

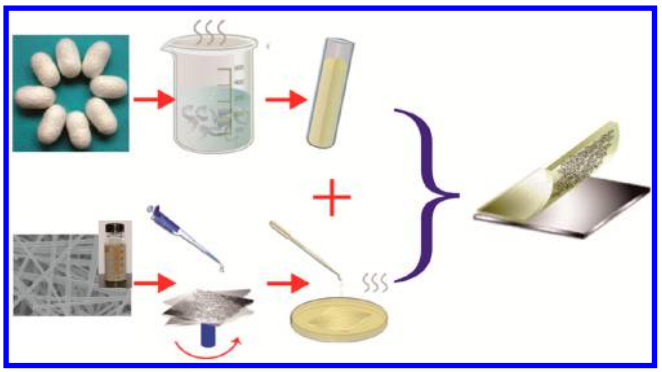

Figure 1. Schematic process of the fabrication of AgNW/SF conductive thin films. (Top) SF was extracted and purified from the silk cocoon. (Bottom) AgNWs were deposited onto a polished silicon substrate by spin-coating and mildly annealing. The aqueous silk fibroin was subsequently poured onto the silicon substrate, and water was allowed to evaporate. Finally, the dry and conductive AgNW/SF film was simply peeled off the silicon substrate.

2.2. Fabrication of Organic Solar Cell. PFN (1-Material) was dissolved in methanol (2 mg/mL) with acetic acid (2 μL/mL), and then spin coated onto the AgNW/SF substrate. PTB7 and $PC_{71}BM$ (1-Material) solutions were prepared according to the report by Liang et al.,[14] and then spin-coated onto the top of the PFN layer at 1000 rpm for 1 min. Finally, a 6 nm-thick MoO_3 layer and a 100 nm-thick AgNW layer were successively deposited through a shadow mask under 10^{-6} Torr (Kurt J. Lesker, Mini Spectra). The device's active area is 7.25 mm^2.

2.3. Characterization of Silk Film and Solar Cell. The transmittance spectrum was measured using a UV–vis spectrophotometer. The resistance was measured using the four-point probe method. The surface morphology and roughness of the substrates were evaluated using an atomic force microscope (AFM). The diameter and distribution of AgNWs were characterized using a scanning electron microscope (SEM). The device performances were characterized under simulated AM 1.5G irradiation at 100 mW/cm^2 using a Xe lamp-based solar simulator.

3. RESULTS AND DISCUSSION

Natural silk displays excellent biocompatibility, biodegradability, and implantability, as well as good mechanical and optical properties. As shown in Figure 1, silk fibers from

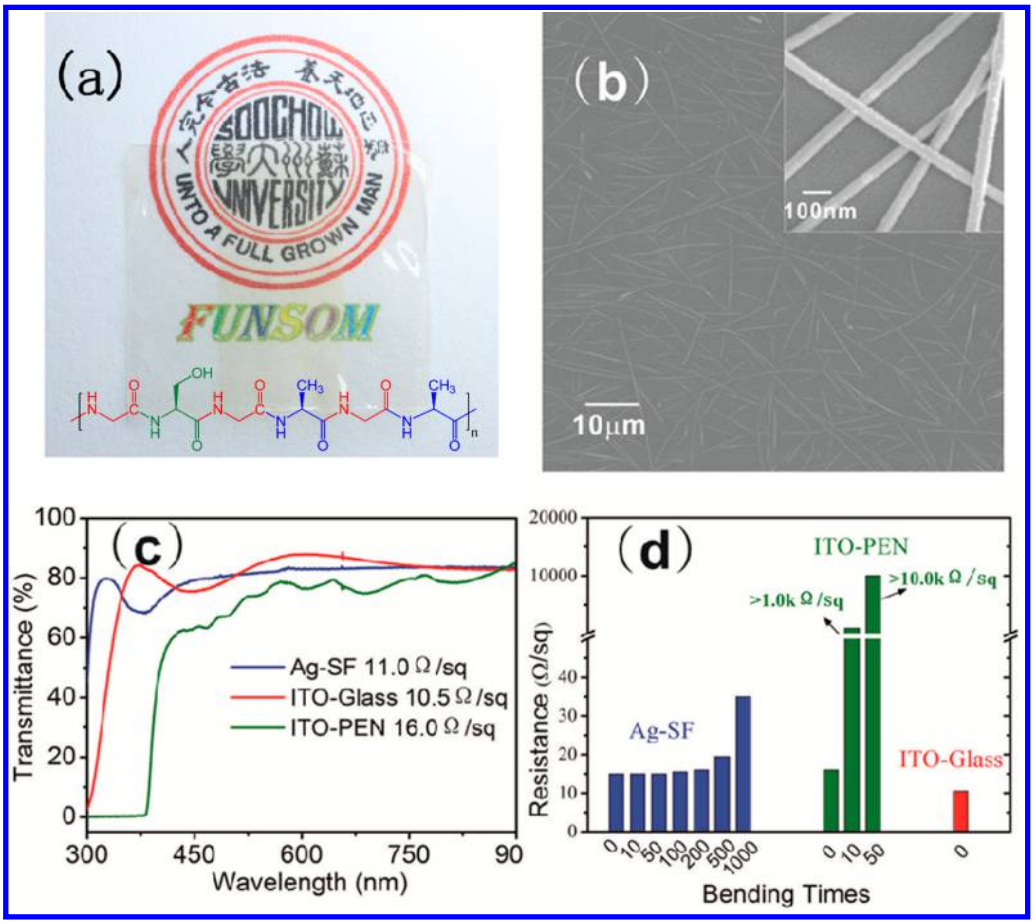

Figure 2. (a) Image of the AgNW/SF substrate; the typical SF molecular internal repeating motif structure is shown at bottom. (b) SEM micrograph of AgNWs embedded in SF film and (inset) high-resolution AgNW mesh. (c) Optical transmittance of the different substrates: ITO-glass, ITO–PEN, and AgNW/SF. (d) The resistance of different conductive substrates before and after the bending test.

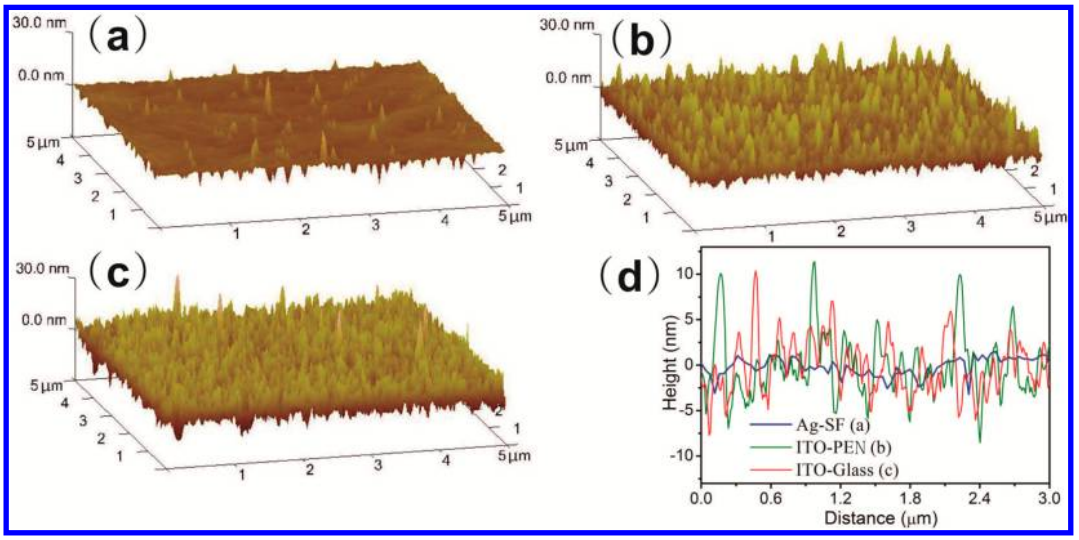

Figure 3. AFM images of roughness on (a) AgNW/SF, (b) ITO−PEN, and (c) ITO glass substrates. (d) Cross-sectional line profile of the topography in each substrate.

silkworm cocoons can be easily processed into films using an aqueous solution. The transformation process begins with boiling the cocoons, then removing impurities. This process yields an aqueous solution of pure SF protein, which can be easily fabricated into a desired thin film shape after the removal of the water. In the experiments, the pristine SF films had thicknesses of ∼20 μm. They displayed a good transparency of approximately 92% across the visible range, as shown in Figure S1 (Supporting Information). This excellent optical transmission is comparable with most commercialized glass and synthetic polymer film (such as polyethylene naphthalate (PEN)), which makes it an excellent candidate in applications requiring a transparent substrate. The high transmittance of the SF film is ascribed to its chemical components, which are mainly composed of a recurring amino acid sequence comprising serine, glycine, and alanine. This sequence is a repeating motif for the typical SF macromolecular structure, as shown in the inset of Figure 2a. These amino acids display weak absorption in the spectra range of 400−1200 nm.

AgNWs networks have been used as transparent conductors due to their high conductivity and optical transmittance.[15,16] In order to form a continuous conductive film on transparent films, AgNWs are usually directly spin- or spray-coated onto the transparent substrate. The film is rough due to the random distribution of AgNWs piling on the substrate. This roughness is a disadvantage because substrate flatness is critical to fabricating the ∼100 nm-thick active layer of the OSC. Additionally, the deposited AgNWs displayed poor adhesion properties on the substrate. To resolve this issue, the AgNWs were first deposited on a flat model substrate instead of being directly deposited onto the substrate. Then, the aqueous SF solution was coated onto the AgNW-covered substrate. When the water was removed after drying, there was a physical adhesion force between SF and AgNW film. In order to ensure that a conductive film would form on the SF substrate, the part of AgNWs that were directly in contact with the silicon substrate were not embedded in SF, as shown in Figure S4b (Supporting Information). Furthermore, the flat model substrate guaranteed the smoothness of the as-prepared conductive films. The AgNW/SF fabrication process is shown in Figure 1. The entire fabrication process took place in all-aqueous conditions at a neutral pH and ambient temperature; these are key conditions when attempting fabrication with biocompatible substrates.

Optical transmittance and substrate conductivity are primary concerns in the performances of OSCs. Varying the thickness of AgNWs requires considering trade-offs between conductivity and transparency. A thinner AgNW layer offers high transparency but poor conductivity; the AgNWs solution must be tuned to achieve an optimized value of both transmittance and conductivity. The longer wires increase the conductivity at the same optical transmittance and then improve the device performance.[15,16] Figure 2a shows an image of a SF substrate embedded with AgNWs. The transmittance of an optimized AgNW/SF substrate is ∼80% in the visible light range, similar to an indium tin oxide (ITO)-coated glass substrate, as shown in Figure 2c. Furthermore, AgNW/SF substrates display an improved transmittance under the ultraviolet spectrum, superior to ITO−PEN. However, there is an obvious absorption peak at 375 nm due to the natural plasmonic effects of AgNWs networks caused by light trapping.[17] The absorption spectrum of AgNWs is plotted in Figure S2 (Supporting Information). The diameter of the AgNWs is between 30 and 40 nm. The AgNWs on the substrate were well-distributed and intercrossed, increasing the current collection area of the AgNW electrodes, as shown in Figure 2b. The resistance of AgNW/SF is ∼11.0 Ω/sq, which is comparable to that of the ITO glass (∼10.5 Ω/sq) substrate.

In order to meet the requirement for flexible OSCs, the substrates must meet certain mechanical requirements to ensure cell stability both during and after the bending process. Figure 2d displays the conductivity of substrates before and after the bending test. When measuring substrate conductivity under the bent condition, the AgNW/SF substrate was bent until one portion folded over another to cover it (bending angle ∼180°), while the ITO−PEN substrate was only bent at a 90° angle. The resistance of the AgNW/SF substrates slightly increases after being bent 500 times but was maintained at below 20 Ω/sq. The ITO−PEN was unable to tolerate the same bending process, with its conductivity increasing to 1000 Ω/sq after being bent just 10 times. The excellent conductivity retention of AgNW/SF following mechanical stress is attributed

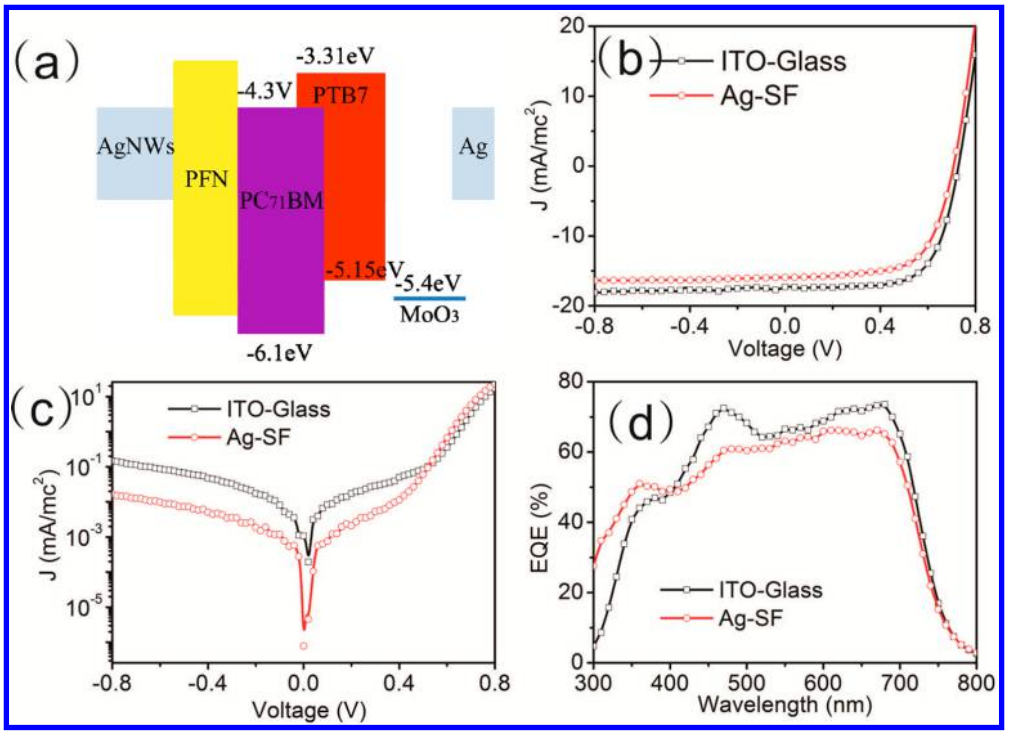

Figure 4. (a) Energy band diagram of the device. (b) $J-V$ curves of the OSCs fabricated on ITO different substrates under AM 1.5G and light intensity of 100 mW/cm^2. (c) $J-V$ curves of the OSCs in the dark. (d) Corresponding EQE curves of OSCs on AgNW/SF and ITO glass substrate.

to the embedded AgNWs in the protein substrate, as well as the ductility of silver (the interfacial structure between AgNWs and SF thin film is shown as Figure S4b, Supporting Information). The slight loss in conductivity may result from the AgNWs drifting during the mechanical bending process. In contrast, ITO films generally displayed fragile properties, showing a quick drop of conductivity after bending. Additionally, the conductivity of AgNW/SF substrates can be recovered after a period of rest ("self-healing");[18] this was attributed to the AgNWs drifting back to their initial positions. For example, AgNW/SF samples that were bent 200 times and then left to recover for 30 min returned to original conductivity. However, the folded ITO−PEN was unable to recover its conductivity even after 1 h of recovery. This indicates that the fragile ITO film is partially broken in the mechanical folding process. In short, the AgNW/SF substrate displayed outstanding flexibility that was superior to the ITO−PEN substrate.

The smoothness of the AgNW network on SF films also plays a critical role in the performance of OSCs. Overly rough morphologies introduce pinholes into the active layer, resulting in increased leakage current that can lead to device failure. AFM images of AgNW/SF, ITO−PEN, and ITO glass are shown in Figure 3. The root-mean-square (RMS) roughness value of the Ag-SF substrates was 1.50 nm, which is much smaller than the values for ITO−PEN (3.38 nm) and ITO glass (4.66 nm). The cross-sectional line profiles of each substrate's topography are also plotted. The height fluctuations of the AgNW/SF substrates were lower than 10 nm, making it smoother than the ITO−PEN or ITO glass substrates. Given these results, the flatness of AgNW/SF substrates meets the requirements of OSCs.

AgNWs networks embedded in SF films exhibit excellent conductivity and transmittance, and were used to fabricate the OSCs. The surface-modified PFN layer was simply spin-coated onto the AgNW/SF substrate according to the previous reports.[12,13] Next, a blend of PTB7 and $PC_{71}BM$ was spin coated onto the PFN layer, forming the active layer. The chemical structures of PFN and PTB7 are shown in Figure S3 (Supporting Information). It should be noted that the entire process did not require any post-treatment such as annealing; this avoided any negative influences on the SF film properties. Furthermore, the back of the SF films did not come in contact with the polymer solution during the entire process, ensuring that properties such as biocompatibility, nontoxicity, and nonirritability were retained on one side of SF thin film. Finally, a 6 nm thick MoO_3 layer and a 100 nm thick AgNW layer were evaporated onto an active layer to fabricate an inverted structure (SF/AgNWs/PFN/(PTB7:$PC_{71}BM$)/MoO_3/Ag) of the flexible OSCs. Figure 4a shows a schematic of the energy levels of the device. PFN acts as a cathode buffer layer to improve the charge collection. PFN can enhance the built-in potential that leads to a higher V_{oc}.[19] PTB7 is used as the electron-donor and $PC_{71}BM$ is the electron-acceptor. Light absorbance and exciton generation take place in the PTB7:$PC_{71}BM$ layer.[12,14,20] Thus, this device shows high lightness and exceptional flexibility.

Figure 4b shows the current density versus voltage ($J-V$) characteristics of OSCs under air mass (AM) 1.5G, at 100 mW/cm^2. An open circuit voltage (V_{oc}) of 0.70 V, a short circuit current density (J_{sc}) of 14.56 mA/cm^2, and a fill factor (FF) of 65% yielded a maximum PCE of 6.62% for the AgNW/SF-based device. An average PCE of 6.07 ± 0.31% was obtained for 12 devices. For comparison, the device fabricated on ITO glass yielded a maximum PCE of 7.89%. The $J-V$ curves of OSCs in the dark are shown in Figure 4b. The figure indicates that the leakage current of AgNW/SF−OSCs is lower than ITO-glass−OSCs, although they did not display a high efficiency. The suppressed leakage current is ascribed to the smooth and flat character of the AgNW/SF substrate, confirming the formation of a dense PFN layer with uniform

coverage. The EQE spectra were consistent with the J_{sc} values of their respective devices, as shown in Figure 4d. A higher EQE was observed for AgNW/SF substrates between 300 and 350 nm; this is ascribed to the higher transmittance of the AgNW/SF substrate. When the obtained device was bent more than 100 times with an angle of ~120°, as shown in Figure 5a, a

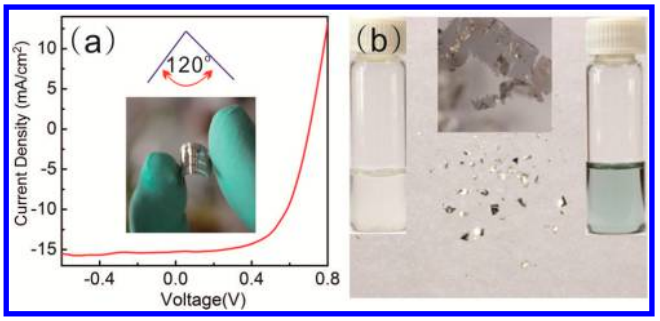

Figure 5. (a) J–V curves of the OSCs with bending angle of ~120°, as shown in the inset image. The bending radius is about 6 mm by bending a 2.7 × 2.7 mm OSC device based on SF/AgNWs thin film. The inset image also exhibits the flexibility of AgNW/SF OSC device. (b) Images of a AgNW/SF-based device degrading process; (inset, left) SF solution obtained by immersing the device in LiBr solution for 1 h at 60 °C and filtering to remove the polymer and the electrode materials (Step 1); (inset, middle) the polymer and the electrode substrate; and (inset, right) conjugate polymer solution obtained by dissolving the polymer and the electrode in chlorobenzene then remove the electrode by filtering (Step 2). The final solid residue was left on a filter paper.

V_{oc} of 0.70 V, a J_{sc} 13.99 mA/cm^2, and a FF of 61% were measured; this yielded a PCE of 5.98%. The good device performance under bending conditions reveals the outstanding flexibility of AgNW/SF-based OSCs.

SF films are fully degradable and dissoluble by the highly concentrated salt solution. Figure 5b shows an image of the degrading device immersed in LiBr aqueous solution and chlorobenzene. These images demonstrated that SF protein is easily dissolved when placed in LiBr solution for 1 h at 60 °C (Step 1). Only the conjugated polymer and the electrode material remain in solution. The remaining solid components were easily removed using filter paper, and the conjugated polymer was dissolved in chlorobenzene (Step 2). After another round of filtration, the silver electrode and MoO_3 were recovered on the filter paper. The aqueous SF solution can be recycled for future fabrication of biocompatible films. On the other hand, the silk fibroin can be easily degraded using enzymes under the appropriate condition.[7−9] Therefore, all of these components (SF, polymer materials, and silver electrode) were easily separated. The easily controlled degradation, biocompatibility and recycling were processed at 60 °C without any other treatment. The degradation and biocompatibility of SF substrate enables silk-based organic devices to be used in a safe manner, opening the doors to the development of a promising class of novel devices.

When considering solar power for portable skin-contact applications, measuring the specific weight in units of Watts per gram is appropriate. Kaltenbrunner et al. recently demonstrated OSCs-on-plastic foil substrates less than 2 μm thick, yielding devices with an extremely high specific weight of 10 W g^{-1}.[21] Here, the thickness of the AgNW/SF film is ~20 μm with a weight of 0.0034 g/cm^2, which is much lighter and thinner than ITO−PEN (~200 μm, 0.028 g/cm^2) and ITO glass substrates (~700 μm, 0.19 g/cm^2). Commercially available high-efficiency Si and triple junction cells can generate 0.676 and 0.360 W g^{-1}, respectively.[22] The OSC constructed on the AgNW/SF presented here can generate 1.71 W g^{-1}. These light, biocompatible, and recyclable devices can be unobtrusively used in natural environments, including on the human body.

4. CONCLUSIONS

In summary, we have demonstrated that flexible and light OSCs with a PCE of 6.62% can be fabricated using SF films as a supporting substrate. These devices displayed excellent degradability in the highly concentrated salty solution. The results show that AgNWs integrated with a SF substrate displayed excellent conductivity, transmittance, and flatness. After extremely rigid bending, the devices retain a stable conductivity that is superior to traditional flexible ITO−PEN substrates. The conductivity of bent AgNW/SF substrates can be recovered via a "self-healing" process. We believe that with continuing efforts in research and development, high-performance SF-based OSCs with exceptional biocompatibility and human affinity will become reality. The realization of SF-based OSCs in commercial and everyday uses promises a bright future for the better interface of the electronics and human beings.

■ ASSOCIATED CONTENT

Ⓢ Supporting Information

The optical transmittance of various substrates, the absorption spectrum of AgNWs film on glass substrate, the chemical structures of PTB7 and PFN molecules, and the patterning of AgNW/SF substrates by the mechanical exfoliation and the SEM micrographs of the interfacial structure. This material is available free of charge via the Internet at http://pubs.acs.org/.

■ AUTHOR INFORMATION

Corresponding Authors

*E-mail: kqzhang@suda.edu.cn. Tel.: +86-512-67061169.
*E-mail: bqsun@suda.edu.cn. Tel.: +86-512-65880951.

Notes

The authors declare no competing financial interest.

■ ACKNOWLEDGMENTS

The authors are grateful for the support from the National Basic Research Program of China (2012CB932402), the National Natural Science Foundation of China (91123005, 61176057, 91027039, 51373110, and 61211130358), the Natural Science Foundation of the Jiangsu Higher Education Institutions of China (10KJA540046), and the Nanotechnology Foundation of Suzhou under Grant ZXG2013037. We also acknowledge support from the Priority Academic Program Development of Jiangsu Higher Education Institutions (PAPD), the Qing Lan Project for Excellent Scientific and Technological Innovation Team of Jiangsu Province (2012), the Project for Jiangsu Scientific and Technological Innovation Team (2013), and the Jiangsu Key Laboratory for Carbon-Based Functional Materials & Devices and Collaborative Innovation Center of Suzhou Nano Science and Technology.

■ REFERENCES

(1) Tang, C. W. Two-Layer Organic Photovoltaic Cell. *Appl. Phys. Lett.* **1986**, *48*, 183.

(2) Yu, G.; Gao, J.; Hummelen, J.; Wudl, F.; Heeger, A. Polymer Photovoltaic Cells: Enhanced Efficiencies Via a Network of Internal Donor-Acceptor Heterojunctions. *Science* **1995**, *270*, 1789−1790.
(3) Krebs, F. C.; Biancardo, M.; Winther-Jensen, B.; Spanggard, H.; Alstrup, J. Strategies for Incorporation of Polymer Photovoltaics into Garments and Textiles. *Sol. Energy Mater. Sol. Cells* **2006**, *90*, 1058−1067.
(4) Altman, G. H.; Diaz, F.; Jakuba, C.; Calabro, T.; Horan, R. L.; Chen, J.; Lu, H.; Richmond, J.; Kaplan, D. L. Silk-Based Biomaterials. *Biomaterials* **2003**, *24*, 401−416.
(5) Lawrence, B. D.; Cronin-Golomb, M.; Georgakoudi, I.; Kaplan, D. L.; Omenetto, F. G. Bioactive Silk Protein Biomaterial Systems for Optical Devices. *Biomacromolecules* **2008**, *9*, 1214−1220.
(6) Jiang, C.; Wang, X.; Gunawidjaja, R.; Lin, Y. H.; Gupta, M. K.; Kaplan, D. L.; Naik, R. R.; Tsukruk, V. V. Mechanical Properties of Robust Ultrathin Silk Fibroin Films. *Adv. Funct. Mater.* **2007**, *17*, 2229−2237.
(7) Jin, H. J.; Park, J.; Karageorgiou, V.; Kim, U. J.; Valluzzi, R.; Cebe, P.; Kaplan, D. L. Water-Stable Silk Films with Reduced B-Sheet Content. *Adv. Funct. Mater.* **2005**, *15*, 1241−1247.
(8) Jin, H.-J.; Park, J.; Valluzzi, R.; Cebe, P.; Kaplan, D. L. Biomaterial Films of *Bombyx Mori* Silk Fibroin with Poly(ethylene oxide). *Biomacromolecules* **2004**, *5*, 711−717.
(9) Rockwood, D. N.; Preda, R. C.; Yucel, T.; Wang, X.; Lovett, M. L.; Kaplan, D. L. Materials Fabrication from *Bombyx Mori* Silk Fibroin. *Nat. Protoc.* **2011**, *6*, 1612−1631.
(10) Wang, C.-H.; Hsieh, C.-Y.; Hwang, J.-C. Flexible Organic Thin-Film Transistors with Silk Fibroin as the Gate Dielectric. *Adv. Mater.* **2011**, *23*, 1630−1634.
(11) Capelli, R.; Amsden, J. J.; Generali, G.; Toffanin, S.; Benfenati, V.; Muccini, M.; Kaplan, D. L.; Omenetto, F. G.; Zamboni, R. Integration of Silk Protein in Organic and Light-Emitting Transistors. *Org. Electron.* **2011**, *12*, 1146−1151.
(12) He, Z.; Zhong, C.; Su, S.; Xu, M.; Wu, H.; Cao, Y. Enhanced Power-Conversion Efficiency in Polymer Solar Cells Using an Inverted Device Structure. *Nat. Photonics* **2012**, *6*, 591−595.
(13) Huang, F.; Wu, H.; Wang, D.; Yang, W.; Cao, Y. Novel Electroluminescent Conjugated Polyelectrolytes Based on Polyfluorene. *Chem. Mater.* **2004**, *16*, 708−716.
(14) Liang, Y.; Xu, Z.; Xia, J.; Tsai, S.-T.; Wu, Y.; Li, G.; Ray, C.; Yu, L. For the Bright Future—Bulk Heterojunction Polymer Solar Cells with Power Conversion Efficiency of 7.4%. *Adv. Mater.* **2010**, *22*, E135−E138.
(15) Zhu, R.; Chung, C.-H.; Cha, K. C.; Yang, W.; Zheng, Y. B.; Zhou, H.; Song, T.-B.; Chen, C.-C.; Weiss, P. S.; Li, G.; Yang, Y. Fused Silver Nanowires with Metal Oxide Nanoparticles and Organic Polymers for Highly Transparent Conductors. *ACS Nano* **2011**, *5*, 9877−9882.
(16) Hu, L.; Kim, H. S.; Lee, J.-Y.; Peumans, P.; Cui, Y. Scalable Coating and Properties of Transparent, Flexible, Silver Nanowire Electrodes. *ACS Nano* **2010**, *4*, 2955−2963.
(17) Guo, C. F.; Sun, T.; Wang, Y.; Gao, J.; Liu, Q.; Kempa, K.; Ren, Z. Conductive Black Silicon Surface Made by Silver Nanonetwork Assisted Etching. *Small* **2013**, *9*, 2415−2419.
(18) Tee, B. C.; Wang, C.; Allen, R.; Bao, Z. An Electrically and Mechanically Self-Healing Composite with Pressure-and Flexion-Sensitive Properties for Electronic Skin Applications. *Nat. Nanotechnol.* **2012**, *7*, 825−832.
(19) He, Z.; Zhong, C.; Huang, X.; Wong, W.-Y.; Wu, H.; Chen, L.; Su, S.; Cao, Y. Simultaneous Enhancement of Open-Circuit Voltage, Short-Circuit Current Density, and Fill Factor in Polymer Solar Cells. *Adv. Mater.* **2011**, *23*, 4636−4643.
(20) Steim, R.; Kogler, F. R.; Brabec, C. J. Interface Materials for Organic Solar Cells. *J. Mater. Chem.* **2010**, *20*, 2499−2512.
(21) Kaltenbrunner, M.; White, M. S.; Głowacki, E. D.; Sekitani, T.; Someya, T.; Sariciftci, N. S.; Bauer, S. Ultrathin and Lightweight Organic Solar Cells with High Flexibility. *Nat. Commun.* **2012**, *3*, 770.
(22) Fatemi, N. S.; Pollard, H. E.; Hou, H. Q.; Sharps, P. R. Solar Array Trades between Very High-Efficiency Multi-Junction and Si Space Solar Cells. In Proceedings of the 28th IEEE Photovoltaic Specialists Conference, Anchorage, AK, Sept 17−22, 2000; The Institute of Electrical and Electronics Engineers: New York,2000; pp 1083−1086.